Pergamon

0301-9322(93)E0018-Z

Int. J. Multiphase Flow Vol. 20, No. 3, pp. 557–568, 1994

0301-9322/94 $7.00 + 0.00

NUMERICAL SIMULATION OF THE PROPAGATION OF SHOCK WAVES IN COMPRESSIBLE OPEN-CELL POROUS FOAMS

M. OLIM,[1]† M. E. H. VAN DONGEN,[2] T. KITAMURA[1] and K. TAKAYAMA[1]

[1]Institute of Fluid Science, Tohoku University, Aoba-ku, Katahira 2-1-1, Sendai 980, Japan

[2]Faculty of Applied Physics, Eindhoven University of Technology, Eindhoven, The Netherlands

(Received 14 April 1993; in revised form 11 November 1993)

Abstract—A numerical model for the simulation of the interaction of weak shock waves with open-cell compressible porous foams is developed. It is assumed that the foam is infinitely weak and that its volume fraction, which was 0.05 in the cases studied herein, is relevant only when the interaction between the gaseous and the solid phases is considered. The gas is assumed to be inviscid and thermally nonconductive, except for the viscous drag interaction and the heat transfer between the two phases. It is also assumed that the heat transfer between the two phases is extremely efficient, i.e. that the heat transfer coefficient is infinitely large. The range of incident shock wave Mach numbers investigated herein is between 1.08 and 1.40, and the range of foam densities is between 14.8 and 57.4 kg/m^3. The numerical results are in very good agreement with experimentally obtained pressure histories and foam particle paths when the incident shock wave Mach numbers are between 1.25 and 1.40 (weak shocks). The agreement between experimentally and numerically obtained pressure histories is poor when the incident shock wave Mach numbers are between 1.08 and 1.18 (very weak shocks). The results of the study indicate that when *weak* shocks interact with open-cell compressible foam, the transfer of momentum between the gaseous and the solid phases is of paramount importance. On the other hand, if the shocks are *very weak*, then the elasticity of the foam is an important parameter as well. It is therefore suggested that, while yielding very good results for *weak* shocks, the assumption of infinitely weak foam is inadequate for *very weak* shocks.

Key Words: compressible foam, shock waves

1. INTRODUCTION

Initial studies of the interaction of shock waves with compressible porous materials were largely motivated by the need to develop methods to attenuate the effects of shock waves upon structures. The research was given considerable impetus when experimental studies indicated that attachment of a layer of compressible foam to a rigid wall results, contrary to initial expectation, in the pressure experienced by the wall being significantly larger, up to a factor of 5, than the pressure developing at the wall in the absence of the foam layer. The study of the processes occurring when a planar shock wave impinges on a porous compressible foam supported by a rigid end wall started with the work of Monti (1970), who established the initial framework for investigation of this phenomenon. Gel'fand *et al.* (1975) evaluated the magnitudes of the pressure increase at the end wall as the wave reflects from it. The theoretical and experimental studies performed since then include those by Gel'fand *et al.* (1983), Henderson *et al.* (1989), Rayevsky *et al.* (1989), Skews *et al.* (1991; Skews 1991), Baer (1992) and van Dongen *et al.* (1993).

Compressible permeable foams exhibit a highly nonlinear stress–strain relation. This behavior is extensively discussed by Gibson & Ashby (1988). At the initial stage of compression the foam structure is unchanged and such foam behaves in a linear elastic manner until the compressive stress reaches a collapse value at which the walls of the foam cells begin to collapse. When the foam is compressed further, the strain increases while the stress remains practically constant at the collapse value. In this regime, the foam cells are partially collapsed and the stress–strain curve displays a plateau. For further compression of the foam the stress is maintained at the collapse value until the foam enters its densification regime. In this regime the foam cells are completely collapsed and the stress–strain curve exhibits a rapid increase in the stress as the foam is compressed. For a typical open-cell compressible foam the intermediate regime, i.e. that of the partially collapsed cells and

†Present address: FSI International, 322 Lake Hazeltine Drive, Chaska, MN 55318, U.S.A.

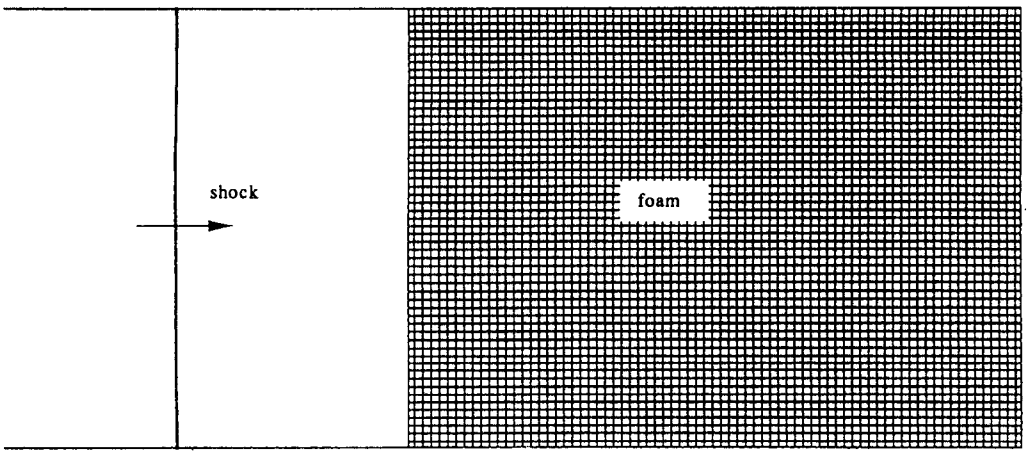

Figure 1. Schematic description of the one-dimensional flow field.

the corresponding plateau in the stress–strain curve, is significantly wider than either of the other two regimes. Thus, when a compression wave which is sufficiently strong so as to induce partial collapse of the foam cells propagates through foam whose cells are filled with gas, it is expected that the foam itself will have but a negligible contribution to the system pressure.

In spite of the ongoing research activity, the reasons for the pressure increase at the rigid wall supporting a layer of compressible foam are not yet fully understood. Numerical studies of the subject are especially impeded by the rather incomplete understanding of the physical processes taking place. One result of this incomplete understanding is that the relative importance of the various processes is unknown. Therefore, numerical simulations must account for the effects of numerous processes often associated with coefficients whose values must be determined empirically. The present study was conducted in order to determine the most important processes taking place during the interaction of shock waves with compressible porous materials. Once these are determined, numerical simulations of such interaction should be capable of delivering reliable predictions at a minimal computational cost.

The flow field of interest is usually assumed to be one-dimensional. Such a flow field is shown schematically in figure 1. The most important feature of the flow field is a layer of porous compressible foam which is supported by a rigid end wall on one side and open to some gas (in the present case this gas is air) on the other side. The pores of the foam are open and full of air. A plane shock wave of given Mach number is propagating in the air towards the foam. This unsteady flow field may be described by a set of conservation equations supplemented by an equation of state for each of the two constituents, i.e. the gas and the foam. In the present study it is assumed that the viscosity and the thermal conductivity of the gas are negligible except for their effect upon drag forces and the heat transfer existing between the two phases. It is also assumed that the foam volume fraction is relevant only when the interaction between the two phases is considered, and that the foam is infinitely weak. The assumption of infinitely weak foam effectively means that no compression waves propagate in the solid material, i.e. the operating regime is that of the plateau in the stress–strain curve. Thus, the contribution of the solid to the system pressure is assumed to be negligible, and the conservation equations describing the flow field may therefore be written as follows:

$$\frac{\partial}{\partial t}\begin{bmatrix}\rho_G\\ \rho_S\\ m_G\\ m_S\\ E_G\\ E_S\end{bmatrix}+\frac{\partial}{\partial x}\begin{bmatrix}m_G\\ m_S\\ u_G m_G+P_G\\ u_S m_S\\ u_G(E_G+P_G)\\ u_S E_S\end{bmatrix}=\begin{bmatrix}0\\ m_G^{\dagger}\\ m_S^{\dagger}\\ e_G^{\dagger}\\ e_S^{\dagger}\\ \end{bmatrix} \qquad [1]$$

or, in vector form,

$$\frac{\partial \mathbf{u}}{\partial t} + \frac{\partial \mathbf{f}}{\partial x} = \mathbf{h}, \qquad [2]$$

where

$$\mathbf{u}^{\mathrm{T}} = [\rho_{\mathrm{G}}, \rho_{\mathrm{S}}, m_{\mathrm{G}}, m_{\mathrm{S}}, E_{\mathrm{G}}, E_{\mathrm{S}}],$$

$$\mathbf{f}^{\mathrm{T}} = [m_{\mathrm{G}}, m_{\mathrm{S}}, m_{\mathrm{G}}u_{\mathrm{G}} + P_{\mathrm{G}}, m_{\mathrm{S}}u_{\mathrm{S}}, u_{\mathrm{G}}(E_{\mathrm{G}} + P_{\mathrm{G}}), u_{\mathrm{S}}E_{\mathrm{S}}]$$

and

$$\mathbf{h}^{\mathrm{T}} = [0, 0, m_{\mathrm{G}}^{\dagger}, m_{\mathrm{S}}^{\dagger}, e_{\mathrm{G}}^{\dagger}, e_{\mathrm{S}}^{\dagger}].$$

The subscripts G and S denote, respectively, the properties of the gaseous and the solid phases, the variables ρ, u, m and E represent the density, velocity, momentum and energy of the constituents. P_{G} is the pressure of the gas, and the energy is defined by $E = \rho(CT + \frac{1}{2}u^2)$, where T and C are the temperature and specific heat at constant volume. The components of the vector $\mathbf{h}$ respresent the interaction between the two phases, $m_{\mathrm{G(S)}}^{\dagger}$ and $e_{\mathrm{G(S)}}^{\dagger}$ being the rates of momentum and energy addition to the gaseous (solid) phase. Clearly, overall conservation of momentum and energy requires that

$$m_{\mathrm{G}}^{\dagger} = -m_{\mathrm{S}}^{\dagger}; \quad e_{\mathrm{G}}^{\dagger} = -e_{\mathrm{S}}^{\dagger}. \qquad [3]$$

Since it is assumed that waves do not propagate in the solid phase a constitutive equation for this phase is no longer required, and since the shock waves studied here are weak the appropriate constitutive equation for the air is the equation of state for a perfect gas, i.e. $P_{\mathrm{G}} = \rho_{\mathrm{G}}\mathrm{R}T_{\mathrm{G}}$. Thus, the system of partial differential equations given by [1] and complemented by the gas equation of state may be solved if the rates of momentum exchange and heat transfer, $m_{\mathrm{G(S)}}^{\dagger}$ and $e_{\mathrm{G(S)}}^{\dagger}$, are defined in terms of the other properties of the flow field.

The precise functional dependency of the rates of momentum exchange and heat transfer between the phases upon the properties of the flow field is yet to be determined theoretically. For the present study, due to the nature of the air flow in the pores of the foam, it is assumed that the heat transfer mechanism between the two phases in extremely efficient, and that the heat conductivity of the foam is sufficiently high to assume a uniform temperature distribution inside the foam. Therefore, where the gaseous and the solid phases coexist they are assumed to be of the same temperature. To evaluate the rate of momentum exchange between the gaseous and the solid phases it is assumed that the friction force is quadratically dependent upon the difference between the velocities of the two phases, i.e. that the rate of momentum exchange may be described by the following equation suggested by van der Grinten *et al.* (1985):

$$m_{\mathrm{S}}^{\dagger} = \phi_{\mathrm{S}}\alpha\mu_{\mathrm{G}}(u_{\mathrm{G}} - u_{\mathrm{S}}) + \phi_{\mathrm{S}}\beta\rho_{\mathrm{G}}(u_{\mathrm{G}} - u_{\mathrm{S}})|u_{\mathrm{G}} - u_{\mathrm{S}}|, \qquad [4]$$

where ϕ_{S} is the volume fraction of the solid phase, μ_{G} is the gas viscosity and α and β are the permeability coefficients. This equation is in agreement with the nonlinear interaction law for porous media known as the Forchheimer relation (Dullien 1979). The values of the permeability coefficients α and β are not known, and steady-state experiments were performed by van Dongen *et al.* (1993) in order to obtain the values of these coefficients. The foams used in their study are not exactly similar to those used herein. Therefore, due to the differences in foams, and to the fact that their experiments were performed in steady flow, their values can only be used as order-of-magnitude estimates. These estimates were refined by comparing numerically obtained pressure signals with the pressure histories recorded in unsteady-state experiments.

2. NUMERICAL METHOD OF SOLUTION

The set of equations describing the flow field, the vector form of which is given by [2], is solved numerically using the operator splitting technique. Thus, assuming that all the flow field properties are known at some given time, [2] is integrated in time by separately solving the homogeneous,

$$\frac{\partial \mathbf{u}}{\partial t} + \frac{\partial \mathbf{f}}{\partial x} = \mathbf{0}, \qquad [5]$$

and the nonhomogenous,

$$\frac{\partial \mathbf{u}}{\partial t} = \mathbf{h}, \qquad [6]$$

parts thereof. The homogeneous part represents the conservative advection and is solved using a Lax–Wendroff method with flux-corrected transport (FCT) developed by Book *et al.* (1975). The nonhomogenous part represents the interaction between the two phases and is solved using a modified Euler method. The FCT method may be implemented with various advection algorithms, and it has been used extensively in simulation of reactive flows [see Oran & Boris (1988) and references therein]. The particular combination of FCT Lax–Wendroff and modified Euler methods employed herein was also tested and employed in the numerical simulation of two-phase flows by Olim *et al.* (1990a,b).

Since it is assumed that the temperature of the solid phase is equal to that of the gas, this temperature may be calculated as an average value weighted by the density and heat capacity of the two phases:

$$T_S = T_G = \frac{\rho_G C_G T_G^* + \rho_S C_S T_S^*}{\rho_G C_G + \rho_S C_S}, \qquad [7]$$

where T_G^* and T_S^* are the temperatures of the gaseous and the solid phases before the process of heat transfer is accounted for. In the present study T_G^* and T_S^* are the temperatures of the two phases obtained from the solution of the vector equation [5]. Skews (1991) states that the sensitivity of the theoretically predicted flow field properties to the specific heat of the foam, C_s, is small. The value used herein for C_S is 1200 J/kg, as suggested by Gel'fand *et al.* (1983), and [7] is solved instead of the last two equations in the vector equation [6].

3. RESULTS AND DISCUSSION

The numerically obtained results are compared with data obtained in shock tube experiments. In all the experiments a block of open-cell foam was inserted into a shock tube so that the foam was in contact with the end wall of the shock tube and also with the four side walls. In order to prevent the propagation of waves between the foam and the shock tube walls, the foam blocks were manufactured so that their cross section is slightly larger than that of the shock tube. Such a snug fit results in friction between the sides of the foam block and the shock tube walls; this friction and its three-dimensional effects were neglected in the one-dimensional numerical simulation.

Skews *et al.* (1991; Skews 1991) reported experimental studies in which several types of foam were used. Foam blocks of various lengths were inserted into a shock tube, and the pressures at various locations along the shock tube were recorded using pressure transducers. A single experiment of another type was reported by Skews *et al.* (1991). In this experiment the motion of the foam was recorded employing high-speed photography, and the velocity of the foam particles was deduced from these recordings. An additional set of experiments, yielding data similar to those obtained in the first set, was carried out with two types of foam at the Shock Wave Research Center of the Tohoku University Institute of Fluid Science. In this set of experiments, the pressures at the end wall of the shock tube were recorded using pressure transducers. Since it is assumed that no waves propagate in the solid phase, the differences between the various types of foam used in these experiments are expressed only by the density of the foam.

In the experiments reported by Skews *et al.* (1991; Skews 1991) the pressure transducers were mounted on the end wall and along one side wall of the shock tube. The incident shock wave Mach numbers (M_i) were 1.25, 1.27, 1.29 and 1.40. The experiments were repeated with various types of foam using foam blocks of various lengths. The pressure signals obtained in some of these experiments and those obtained numerically are compared in figures 2–5. In the experiments whose results are shown in figures 2–4, the pressure transducers are numbered from 1 to 4, and their distances from the end wall are, respectively, 320, 220, 120 and 0 mm. Thus, transducer number 4 is located at the end wall. In the experiment whose results are shown in figure 5, the pressure transducers are numbered from 1 to 3, and their distances from the end wall, are, respectively, 103, 43 and 0 mm (with transducer 3 at the end wall). In all the experiments the volume fraction of the solid foam is 0.05.

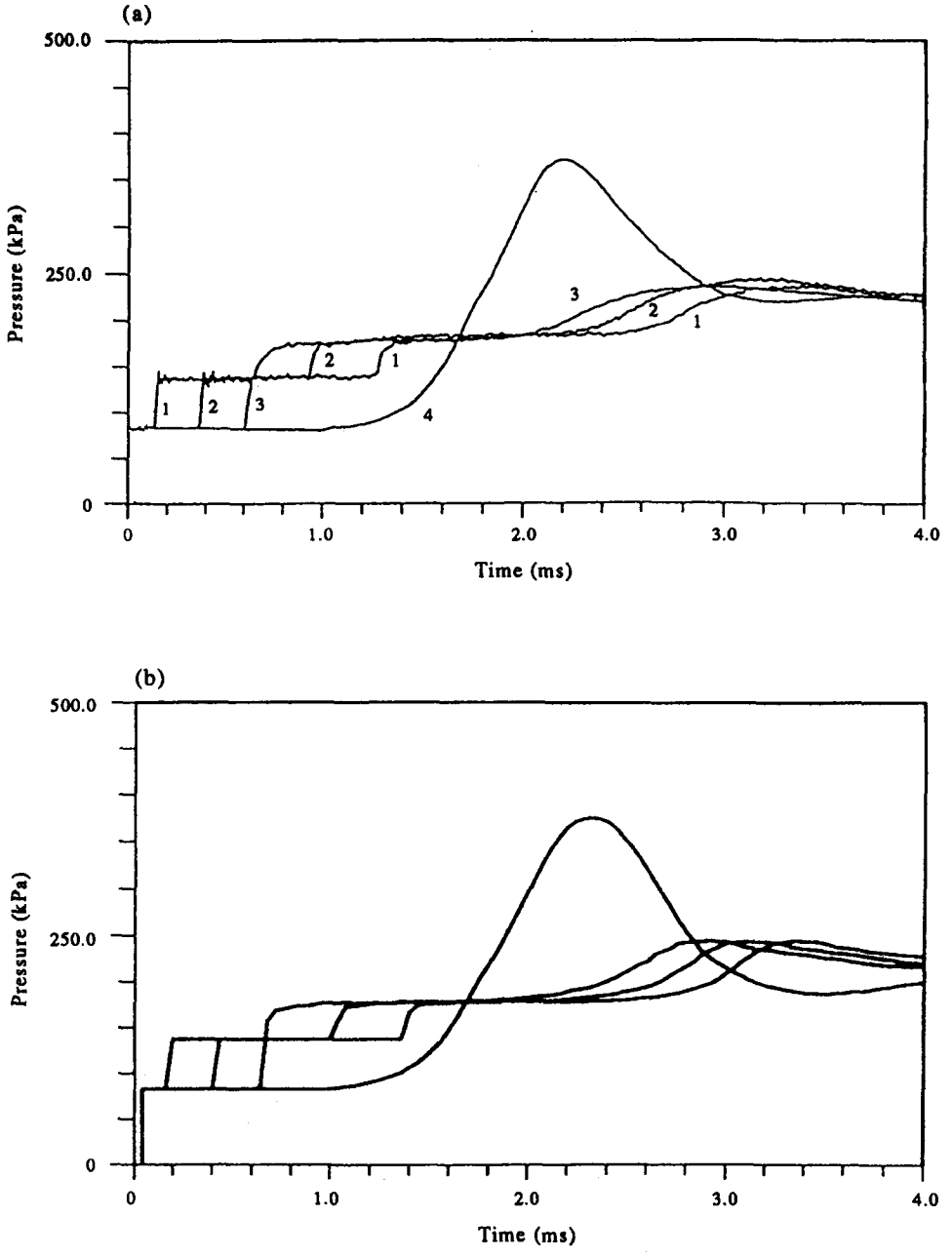

Figure 2. Experimentally (a) and numerically (b) obtained pressure histories for $M_i = 1.25$, $\rho_s = 14.8\ kg/m^3$. The experimental results are reproduced with permission from Skews (1991).

In the experiments, the shock wave is generated in a shock tube and initially propagates in air. At a later stage the shock wave interacts with the interface between the air and the foam, thus generating two waves: one reflecting back into the air and the other propagating into the porous foam. The shock propagating into the foam is dampened due to the interaction between the two phases and it exhibits dispersion, as demonstrated by van Dongen *et al.* (1993). The strong pressure increase observed at the end wall is a result of the reflection of the dispersed wave from that wall. Due to the dispersion of the wave propagating in the foam the pressure transducers located between the air–foam interface and the end wall record a gradual increase in pressure as opposed to the sudden pressure jump recorded by the pressure transducers located in the air.

Figure 2(a) shows the pressure histories obtained experimentally for an incident shock wave of $M_i = 1.25$ impinging upon a 120 mm long block of polyether foam whose density is 14.8 kg/m^3, and figure 2(b) shows the corresponding pressure histories obtained numerically. The shock wave passes transducers 1 and 2 before reaching the air–foam interface and, accordingly, these transducers show sudden pressure jumps. Transducer 3 is located in the very vicinity of the interface and shows a rapid but not an immediate pressure increase. Transducer 4 is located at the end wall and shows a gradual pressure increase. The pressure histories also show the somewhat dispersed waves reflected by the interface and the severely dispersed waves reflected by the end wall as they reach transducers 3, 2 and 1. Figures 3(a) and (b) show, respectively, the experimentally and numerically obtained pressure histories for an incident shock wave of $M_i = 1.27$ impinging upon a 50 mm long

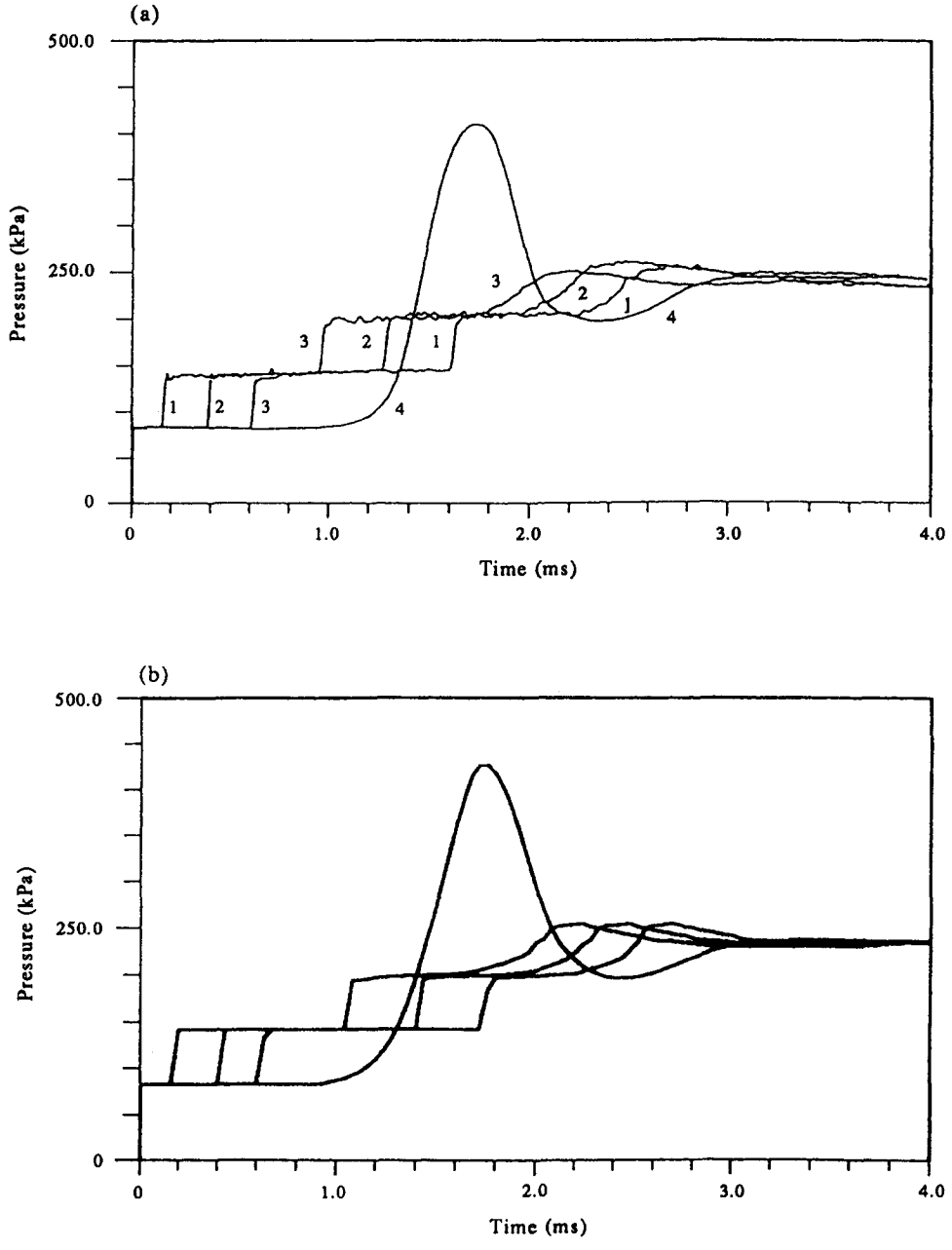

Figure 3. Experimentally (a) and numerically (b) obtained pressure histories for $M_i = 1.27$, $\rho_s = 35.0$ kg/m^3. The experimental results are reproduced with permission from Skews (1991).

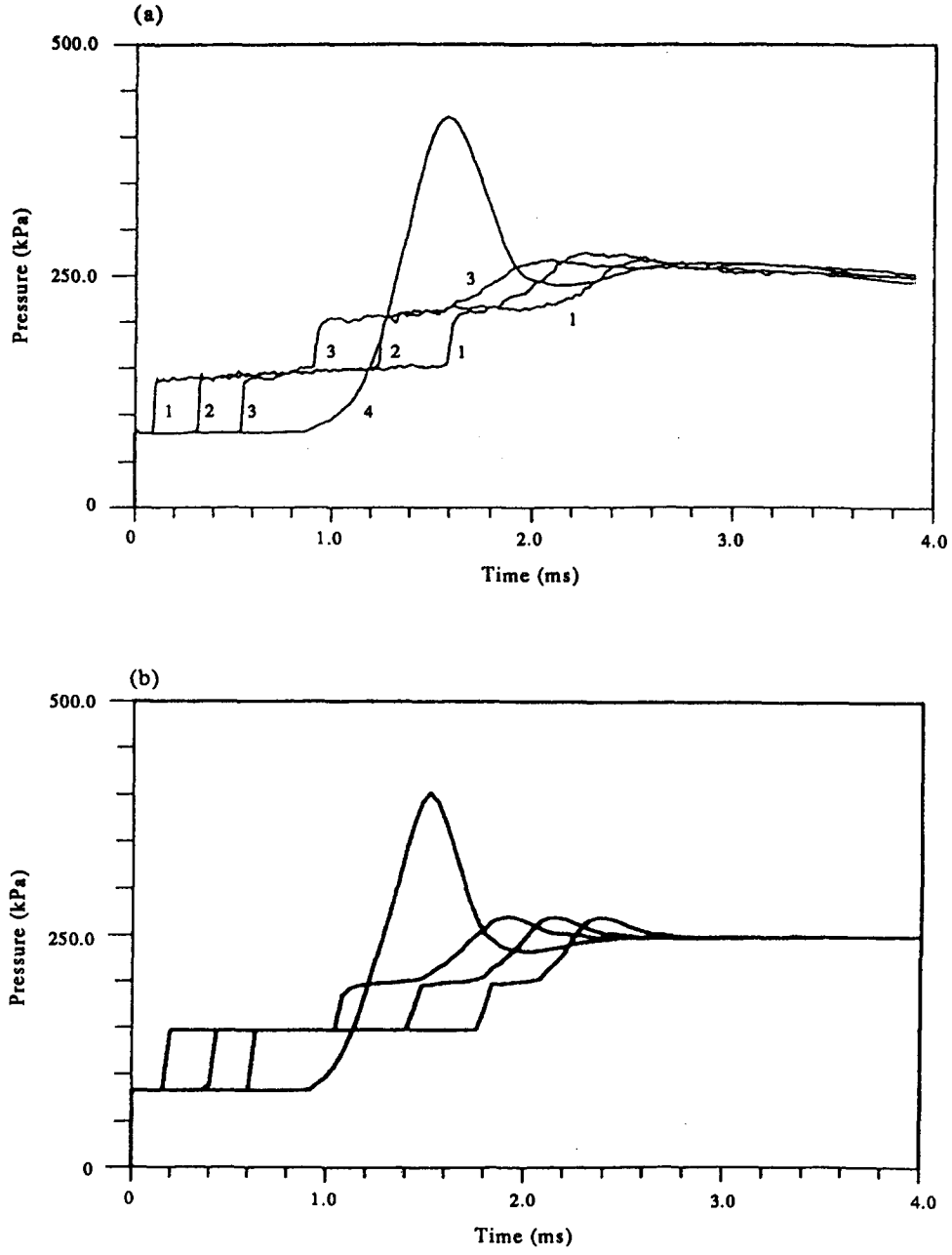

Figure 4. Experimentally (a) and numerically (b) obtained pressure histories for $M_i = 1.29$, $\rho_s = 18.7\ kg/m^3$. The experimental results are reproduced with permission from Skews (1991).

block of polyester foam whose density is 35.0 kg/m^3. Transducers 1–3, which are located in the air, show initially the pressure jumps as the shock passes over them and later the waves reflected by the interface and the end wall. Transducer 4 shows the dispersed pressure wave at the end wall. Figures 4(a) and (b) show, respectively, the experimentally and numerically obtained pressure histories for an incident shock wave of $M_i = 1.29$ impinging upon a 50 mm long block of polyester foam whose density is 18.7 kg/m^3. The wave characteristics are similar to those observed in the previous experiment. Figures 5(a) and (b) show, respectively, the experimentally and numerically obtained pressure histories for a shock wave of incident $M_i = 1.40$ impinging upon a 70 mm long block of polyester foam whose density is 38.0 kg/m^3. Pressure transducer 1 is located in the air and shows the pressure jump and the less rapid pressure increase corresponding, respectively, to the

incident shock and to the wave reflected from the air–foam interface. Transducer 2 is located in the foam and shows a gradual pressure increase caused by the dispersed wave propagating in the foam. Transducer 3 shows the gradual pressure increase at the end wall. The dispersed wave reflected from the end wall is also recorded by transducers 2 and 1. The agreement between the numerically and experimentally obtained pressure histories is very good except for the last case in

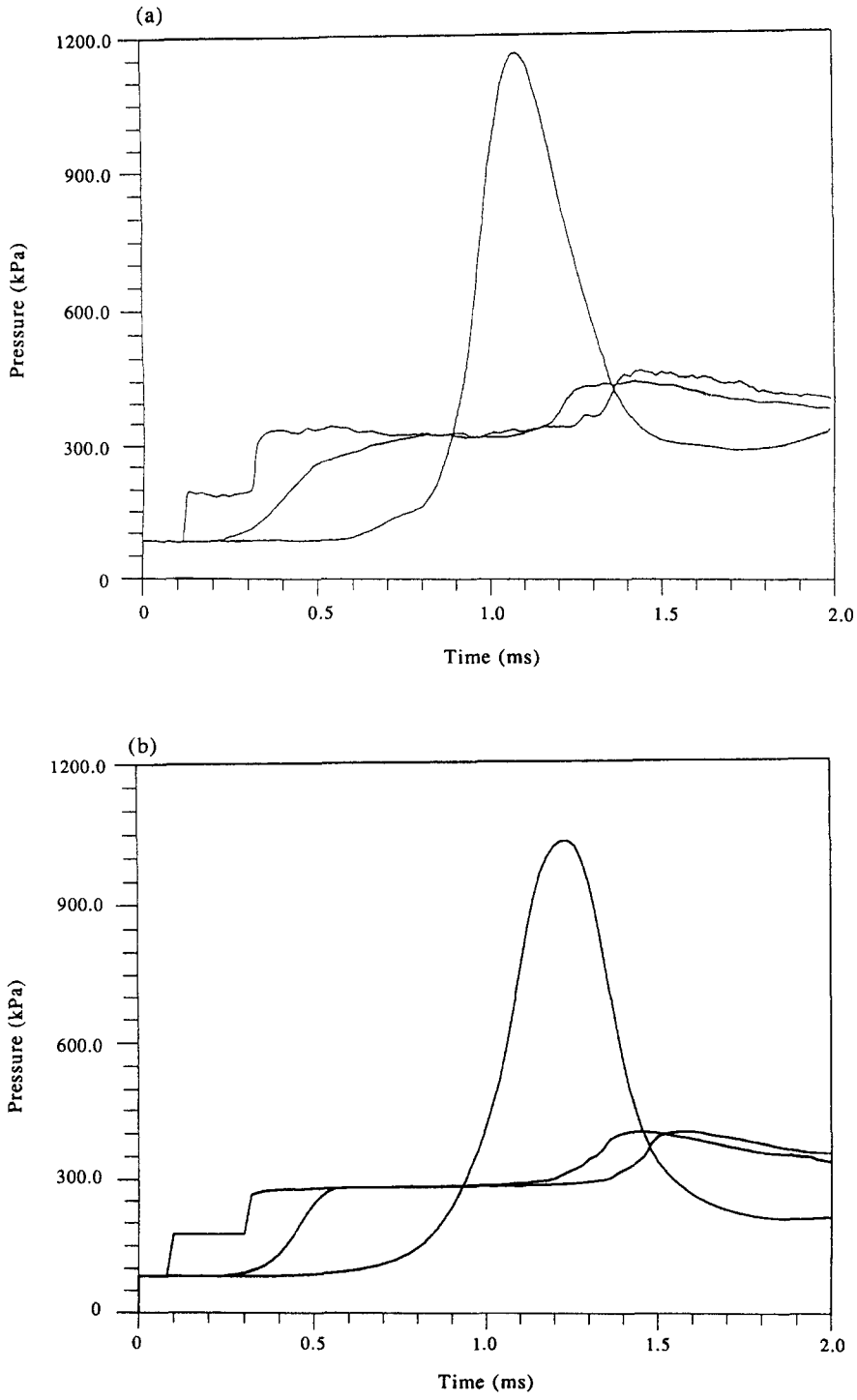

Figure 5. Experimentally (a) and numerically (b) obtained pressure histories for $M_i = 1.40$, $\rho_s = 38.0\,kg/m^3$. The experimental results are reproduced with permission from Skews *et al.* (1991).

which the numerically obtained pressure at the end wall is somewhat lower than that observed experimentally.

In the single experiment of the second type reported by Skews *et al.* (1991), a pattern was painted on one side of the foam block thus enabling the use of high-speed photography to record the positions of various foam particles. These photographic recordings were used for reconstruction of the motion of the foam particles. The incident shock wave Mach number in this experiment was 1.40. The experimentally obtained particle paths for a 70 mm long block of polyether foam whose density and volume fraction are, respectively, 32.5 kg/m^3 and 0.05 are compared to those obtained numerically in figures 6(a) and (b). Again, the agreement between the numerically and experimentally obtained data is very good. For example, Skews (1991) reports that in the initial part of the reflection process the velocity of the air–foam interface deduced from the experimental data is approximately 55 m/s, and that a wave is traveling through the foam at velocity of approximately 90 m/s. The corresponding values deduced from the numerical data are approximately 62 and 105 m/s. The fact that the numerically obtained values of the interface velocity and of the wave speed are somewhat higher than their experimentally determined values may possibly be attributed to the effects of wall friction, which are neglected in the simulation.

In each numerical experiment the values of the permeability coefficients obtained in the steady-state experiments were optimized for good agreement with the experimental results. To achieve this agreement the permeability coefficients obtained from the steady-state experiments were multiplied by a factor which varied between 5 and 8. No such factors were found to yield good agreement of the numerical and experimental result for the very weak shocks. This is most likely due to the fact that very weak shocks did not compress the foam beyond its collapse point,

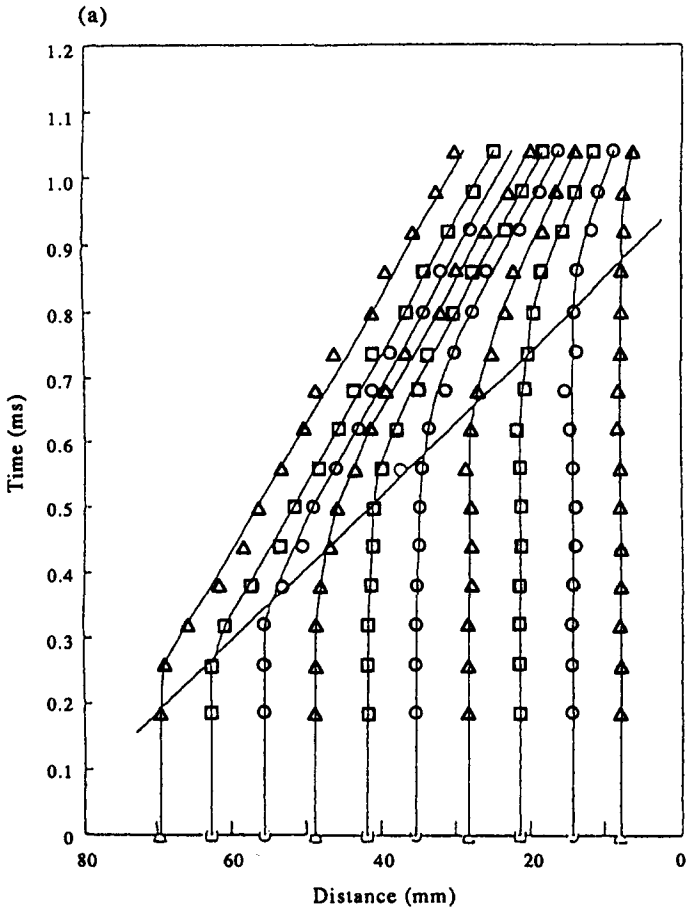

Fig. 6(a). *Caption overleaf.*

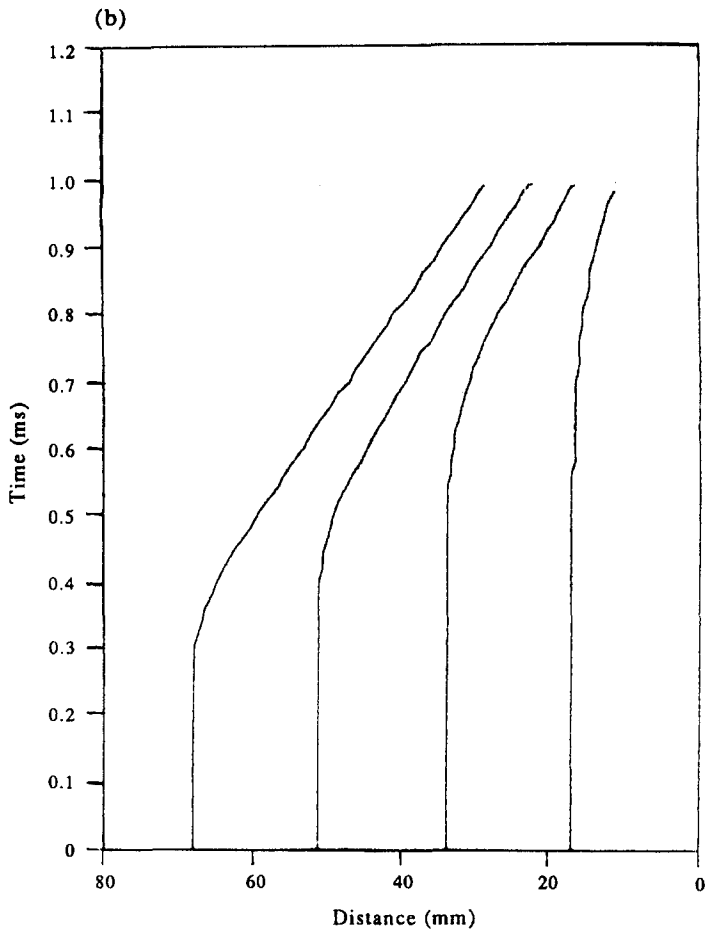

Fig. 6(b)

Figure 6. Experimentally (a) and numerically (b) obtained particle paths for $M_i = 1.40$, $\rho_s = 32.5\ kg/m^3$. The experimental results are reproduced with permission from Skews *et al.* (1991).

thus contradicting one of the main assumptions, i.e. that of infinitely weak foam. The fact that the steady-state values of permeability coefficients had to be increased in order to obtain good agreement between the experimental and numerical data indicates that the drag force which exists between the two phases in an unsteady flow is higher than that in the steady state. The increase in the drag force is consistent with the increase known to exist between the steady and unsteady drag coefficients of spherical particles submerged in a fluid [see, for example, the paper by Rudinger (1980)]. This increase may therefore be partially attributed to the unsteadiness of the flow and partially to the types of foam used by Skews, the permeability coefficients of which are not specified and may be higher than those obtained by van Dongen *et al.* (1993). It is important to notice that the numerically obtained values of the permeability coefficients for accelerating foam are robust in the sense that their variations are relatively small for a fairly wide range of incident shock wave Mach numbers and foam densities.

Clearly, the assumption of infinitely weak foam is valid only if the incident shock wave is sufficiently strong so as to exert upon the foam a stress capable of compressing it beyond the collapse point. In order to estimate the lower boundary of the incident shock wave Mach number value for which the assumption of infinitely weak foam is still valid, an additional set of experiments was performed at the Shock Wave Research Center of the Tohoku University Institute of Fluid Science. In these experiments the pressure transducers were mounted on the end wall of the shock tube. The incident shock waves were of $M_i = 1.08$ and 1.18 (very weak shocks). The two types of foam used in these experiments were moltopren Pu-Sc and Pu-Sm-65. Their densities were 28.8 and

57.4 kg/m^3, and their respective volume fractions were 0.023 and 0.047. The lengths of the foam blocks were 70 and 140 mm. The agreement between the numerically and experimentally obtained results with an incident shock wave of $M_i = 1.18$ was poor, and the agreement for an incident shock wave of $M_i = 1.08$ was poorer still. The experimentally obtained pressure histories for these very weak shocks exhibit a far better agreement with the results predicted analytically by van Dongen *et al.* (1993), who linearized the equations of conservation of mass and momentum, and assumed that the foam is completely elastic. The most significant difference between the assumptions employed in the linear analytical study carried out by van Dongen *et al.* (1993) and those employed in the present numerical model is that in the former case the foam is assumed to be completely elastic, while in the latter case the foam is assumed to be infinitely weak. It is therefore concluded that, for the types of foam considered herein, the lowest incident shock Mach number for which the assumption of infinitely weak foam is valid is between 1.18 and 1.25, while the highest is approximately 1.40.

The set of experiments reported by Skews (1991), i.e. that in which pressure histories were recorded for various foams and incident shock wave Mach numbers, was also simulated numerically by Baer (1992). In Baer's model the volume fraction of the solid phase was accounted for in the simulation of the advection process, and the simulated physical processes included a compaction model for the foam. The closure of the set of equations was achieved by using a thermoelastic equation of state for the foam. In spite of the complicated physical processes which were accounted for, the results of this numerical simulation show only a qualitative agreement with experimental results. Our numerically obtained results, on the other hand, exhibit good agreement with those obtained experimentally for weak incident shock waves. This clearly indicates that, when the shocks are sufficiently strong so as to compress the foam pores beyond the collapse point, the momentum exchange between the two phases is of paramount importance while the process of foam compression and the temperature distribution inside the solid phase have but minor effects on the phenomenon of interaction of weak shock waves with open-cell compressible porous foams. The poor agreement obtained for *very weak* shocks, on the other hand, indicates that the elasticity of the foam is an important parameter in the regime of very weak shocks.

4. CONCLUSIONS

A numerical model for the simulation of the propagation of weak shock waves in open-cell compressible porous foams was developed. It is assumed that the foam is infinitely weak and that its volume fraction is relevant only when the interaction between the gaseous and the solid phases is considered. The gas is assumed to be inviscid and thermally nonconductive, except when the viscous drag interaction and heat transfer between the two phases are considered. It is also assumed that the heat transfer between the two phases is extremely efficient. The assumption of infinitely weak foam is valid when the foam is, on the one hand, compressed beyond its collapse point but, on the other hand, its pores have not yet fully collapsed. The range of Mach numbers investigated is between 1.08 and 1.40, and the range of foam densities is between 14.8 and 57.4 kg/m^3. The foam volume fraction is 0.05. The agreement between the numerically and experimentally obtained results for *weak* incident shocks ($M_i \leqslant 1.18$) is poor, while the agreement between the numerically and experimentally obtained results for *weak* incident shocks ($M_i = 1.25$ to 1.40) is very good. Due to the very good agreement between the numerically and experimentally obtained results, it is concluded that for the cases studied here the interaction of *weak* shock waves with open-cell compressible foams may be accurately modeled using the assumptions of an infinitely weak foam, an infinitely large heat transfer coefficient and neglecting the volume fraction of the solid phase in the simulation of the advection process. It is also concluded that the assumption of an infinitely weak foam is inadequate for the numerical simulation of the interaction of *very weak* shock waves with open-cell compressible foams. The results of the study indicate that for weak shocks in compressible foam the transfer of momentum between the two phases is of paramount importance, while the effects of foam compression and temperature distribution inside the solid phase are relatively minor. It is therefore suggested that, in order to improve the numerical simulation of that phenomenon, it is necessary to compile a database of permeability coefficients for various types

of foam. This data will enable the numerical simulation of the propagation of weak shock waves in compressible foam to deliver reliable predictions at a minimal computational cost.

Acknowledgement—The authors are grateful to B. W. Skews for his permission to use the experimental results.

REFERENCES

BAER, M. R. 1992 A numerical study of shock wave reflections on low density foam. *Int. J. Shock Waves* **2,** 121–124.

BOOK, D. L., BORIS, J. P. & HAIN, K. 1975 Flux corrected transport 2. Generalisation of the method. *J. Comput. Phys.* **18,** 248–283.

VAN DONGEN, M. E. H., SMEULDERS, D. J. J., KITAMURA, T. & TAKAYAMA, K. 1993 On wave phenomena in permeable foam. Report from the Institute of Fluid Science, Tohoku Univ., Sendai, Japan, pp. 55–68.

DULLIEN F. A. L. 1979 *Porous Media*, pp. 195–197. Academic Press, London.

GEL'FAND, B. E., GUBIN, S. A., KOGARKO, S. M. & POPOV, O. E. 1975 Investigation of propagation and reflection of pressure waves in porous media. *Zh. Prikl. Mekh. Tekh. Fiz.* **16,** 74–77.

GEL'FAND, B. E., GUBONOV, A. V. & TIMOFEEV, E. J. 1983 Interaction of shock waves in air with porous screen. *Mekh. Zhid. Gaza* **4,** 78–84.

GIBSON, L. J. & ASHBY, M. 1988 *Cellular Solid Structure and Properties*. Pergamon Press, Oxford.

VAN DER GRINTEN, J. G. M., VAN DONGEN, M. E. H. & VAN DER KOGEL, H. 1985 A shock tube technique for studying pore pressure propagation in a dry and water-saturated medium. *J. Appl. Phys.* **58,** 2937–2942.

HENDERSON, L. F., VIRGONA, R. J., DI, J. & GVOZDEVA, L. G. 1989 Refraction of a normal shock wave from nitrogen into polyurethane foam. In *Current Topics in Shock Waves* (Edited by KIM, Y. W.), pp. 814–818. Springer, Berlin.

MONTI, R. 1970 Normal shock wave reflection on deformable solid walls. *Meccanica* **4,** 285–296.

OLIM, M., IGRA, O., MOND, M. & BEN-DOR, G. 1990a Numerical investigation of the flow behind a shock wave propagating into a carbon-oxygen suspension. *Phys. Fluids A* **2,** 1393–1403.

OLIM, M., BEN-DOR, G., MOND, M. & IGRA, O. 1990b A general attenuation law of moderate planar shock waves propagating into dusty gases with relatively high loading ratios of solid particles. *Fluid Dynam. Res.* **6,** 185–200.

ORAN, E. S. & BORIS, J. P. 1988 *Numerical Simulation of Reactive Flow*. Elsevier, New York.

RAYEVSKY, D. K., GVOZDEVA, L. G. & FARESOV, Y. 1989 Reflection of shock and explosion waves from surfaces covered with layers of polyurethane foam. Presented at the *12th Int. Colloq. on Dynamics of Explosions and Reactive Systems*, Univ. of Michigan, Ann Arbor, MI.

RUDINGER, G. 1980 *Fundamentals of Gas–Particle Flow*. Elsevier, Amsterdam.

SKEWS, B. W. 1991 The reflected pressure field in the interaction of weak shock waves with a compressible foam. *Int. J. Shock Waves* **1,** 205–211.

SKEWS, B. W., ATKINS, M. D. & SEITZ, M. W. 1991 Gas dynamic and physical behavior of compressible foam struck by a weak whock wave. Presented at the *18th Int. Symp. on Shock Waves*, Sendai, Japan (1991).